




ORIGINAL ARTICLE

Open Access



New sesquiterpenoids with anti-inflammatory effects from phytopathogenic fungus *Bipolaris sorokiniana* 11134

Qiang Yin^{1†}, Jianying Han^{1,2,3†}, Guixiang Yang¹, Zhijun Song⁴, Keke Zou¹, Kangjie Lv¹, Zexu Lin¹, Lei Ma¹, Miaomiao Liu², Yunjiang Feng², Ronald J. Quinn², Tom Hsiang⁵, Lixin Zhang¹, Xueting Liu¹, Guoliang Zhu^{1*}  and Jingyu Zhang^{1*}

Abstract

Sesquiterpenoids represent a structurally diverse class of natural products widely recognized for their ecological significance and pharmacological potential, including antimicrobial, anti-inflammatory, and anticancer properties. As part of our efforts to explore bioactive secondary metabolites from phytopathogenic fungi, we conducted a molecular networking-based analysis of *Bipolaris sorokiniana* isolate BS11134, which was fermented on a rice medium. This analysis led to the identification of three new seco-sativene-type sesquiterpenoids (**1–3**) and seven known analogues (**4–10**), with the NMR data of compound **4** being reported for the first time. The structures of these compounds were elucidated using HR-ESI-MS and extensive spectroscopic data analysis. Notably, compound **9** significantly inhibited nitrous oxide expression in lipopolysaccharide (LPS)-treated RAW264.7 cells in vitro (inhibition rate: $84.7 \pm 1.7\%$ at $10 \mu\text{M}$), while compound **1** ($10 \mu\text{M}$) showed a weak inhibitory effect (inhibition rate = $28.0 \pm 2.4\%$). Additionally, we proposed a biosynthetic pathway for these compounds. This study not only expands the chemical space of the helminthoporene class of molecules but also underscores the untapped potential of phytopathogenic fungi as promising sources of structurally unique and biologically active natural products.

Keywords Phytopathogenic fungi, *Bipolaris sorokiniana* 11134, Sesquiterpenoid, Anti-inflammatory

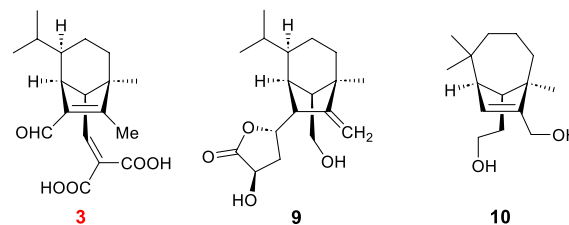
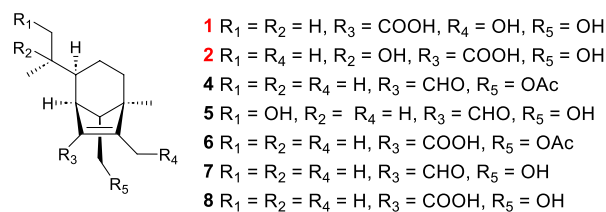
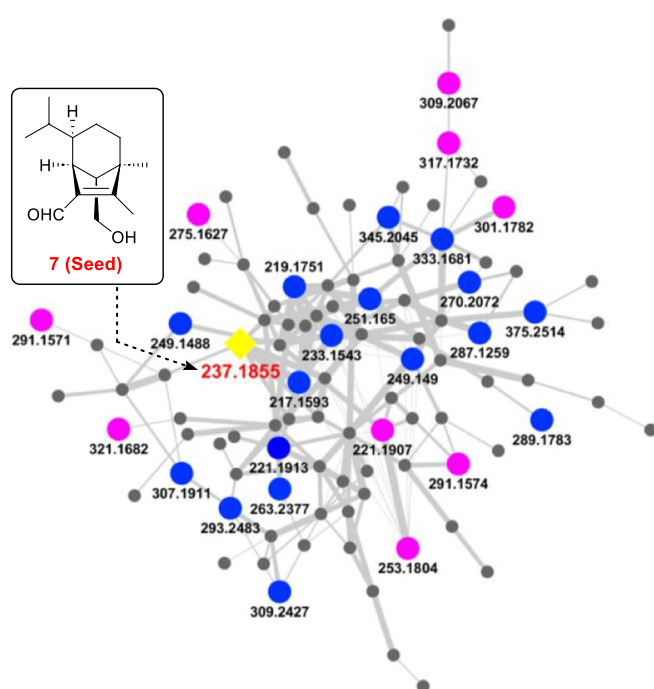
[†]Qiang Yin and Jianying Han contributed to this work equally.

*Correspondence:

Guoliang Zhu
zhuguoliang@ecust.edu.cn
Jingyu Zhang
zhangjingyu@ecust.edu.cn

Full list of author information is available at the end of the article

Graphical Abstract



NO Inhibitory Activity

Compound	% NO inhibition (10 μ M)
1	28.0 \pm 2.4
2	10.9 \pm 2.3
8	14.4 \pm 2.5
9	84.7 \pm 1.7
Indomethacin	51.2 \pm 2.0

1 Introduction

Inflammation in animal tissues is a complex reaction regulated by several inflammatory mediators, including nitric oxide (NO), prostaglandins E2, cytokines, and growth factors [1]. Inflammation is commonly associated with various pathophysiological conditions, such as arthritis, tumours, Alzheimer, or cardiovascular diseases [2–4]. Macrophages, pivotal in host defence, release inflammatory mediators upon activation by lipopolysaccharides (LPS), contributing to pathogenesis. Thus, inhibition of macrophage-produced mediators may attenuate the development of related diseases.

Sesquiterpenes play significant roles in biology and ecology [5], displaying a range of activities in fighting against tumors, viruses, fungi, HIV, biotic pressures, immunity issues, and pests [6–13].

Fungi, especially those interacting with plants, are a rich source of novel sesquiterpenes [14, 15]. Based on cross-talk between plants and phytopathogens, phytopathogenic fungi can co-evolve with host plants, which leads to the production of unique natural products. Phytopathogenic fungi are a source for the discovery of new active compounds.

Traditionally, the isolation of secondary metabolite (SMs) has relied on bioactivity-directed isolation or via

screening targets with distinct spectroscopic features. Recently, Molecular Networking (MN) has revolutionized the visualization of chemical diversity of extracts through the spectral alignment of tandem mass spectrometry (MS^b) data, which captures in-source fragmentation and ionization patterns [16, 17]. MN is particularly adept at identifying unclassified molecules that may hold biological significance or represent novel metabolic pathways, especially useful in comparative studies of different states, such as time points or genetic variant [18]. To enhance the capabilities of MN, Feature-based molecular networking (FBMN) was introduced in 2020, offering enhanced functionality by incorporating chromatographic feature detection into spectral alignment [19].

Bipolaris sorokiniana, a well-known phytopathogenic fungus, causes diseases of barley and wheat, such as root rots, leaf spots, seedling blight, and head blight [20]. Known for producing a range of phytotoxic substance [21, 22], this fungus has been linked to approximately 20 sesquiterpenoids related to helminthosporol across different *Bipolaris* species. In this study, we report the discovery of ten sesquiterpenoids (**1–10**) from *B. sorokiniana* with a helminthoporene skeleton. This included the identification of three new *seco*-sativene type compounds

(1–3) through Global Natural Product Social (GNPS) molecular networking and LC–MS/MS analysis. Additionally, we assessed the anti-inflammatory potential of these isolated sesquiterpenoids in vitro, focusing on their capacity to inhibit NO production induced by LPS in the cell lines of RAW264.7.

2 Results

2.1 Sesquiterpenoids gene clusters exploration from BS11134 based on genome analysis

BS11134 was classified as *Bipolaris sorokiniana* based on morphology and sequence of the internal transcribed spacer (ITS) region (GenBank accession number KU297882) [23]. We used the Hidden Markov Models file (Terpene_syn_C_2) classified in the Pfam database [24] to examine the BS11134 genome obtained in our previous study [23] for potential sesquiterpene cyclase (STC) genes, resulting in four homologous sequences of known STC proteins with DDXXD metal binding motifs. Further annotation of these four STC-encoding biosynthetic gene clusters using antiSMAS [25] and 2ndfinder online software revealed various post-modification enzymes, including cytochrome P450, acetyltransferase, decarboxylase, etc. (Fig. 1). Notably, the length of STC8 gene cluster was only 15 kb (Fig. 1), consisting of a three-gene cassette very similar to the recently identified *seco*-sativene gene cluster [26].

2.2 FBMN guided detection of sesquiterpenoids

We used rice medium to ferment the fungus because this medium gave the most induced secondary metabolites compared with other six media used [23]. A previously reported *seco*-sativene type sesquiterpenoid

helminthosporol (7) was characterized from the crude extract of BS11134 based on its UV spectrum and HR-MS data (Fig. 2B and Fig. S7a). Further analysis using GNPS FBMN identified new *seco*-sativene type sesquiterpenoids using helminthosporol (7) as the seed compound (Fig. 2A), the precursor m/z of 7 was found to be within Cluster I, comprising 97 nodes with similar MS/MS patterns.

Detailed HRESIMS data annotation (Table 1) revealed 27 potential sesquiterpenoids, ten of which showed similar UV spectra to helminthosporol in the HPLC chromatogram of subfraction RD3. Among these, five nodes exhibited previously unreported m/z values (291.1571, 291.1574, 321.1682, 301.1782, 253.1804), guiding the isolation of new sesquiterpenoids from several subfractions. Three new sesquiterpenoids (1–3) with a helminthoporene skeleton as well as seven known compounds (4–10) were identified (Fig. 2C).

2.3 Structure elucidation of isolated sesquiterpenoids

The molecular formula of compound 1 was $C_{15}H_{24}O_4$ confirmed by its HRESIMS data ($[M+Na]^+$ m/z 291.1567, calcd. for $C_{15}H_{24}O_4Na^+$ 291.1571) (Fig. S1a). Analysis of 1H NMR, ^{13}C NMR, and HSQC spectra (Table 2 and Figs. S1b–S1d) revealed a carboxyl cluster [δ_C 167.5], two olefinic carbons [δ_C 157.7, 128.5], four methylene (two of which were substituted with the hydroxyl groups [δ_C 55.6, 59.9]), four methine and three methyl groups, as well as one sp^3 quaternary carbon, outlining a *seco*-sativene sesquiterpene skeleton. The 1H - 1H COSY (Fig. S1e) revealed a continuous spin system extending from H_2 –4 to H_3 –10/ H_2 –11. In addition, H-6 was further coupled with H-7, which also coupled

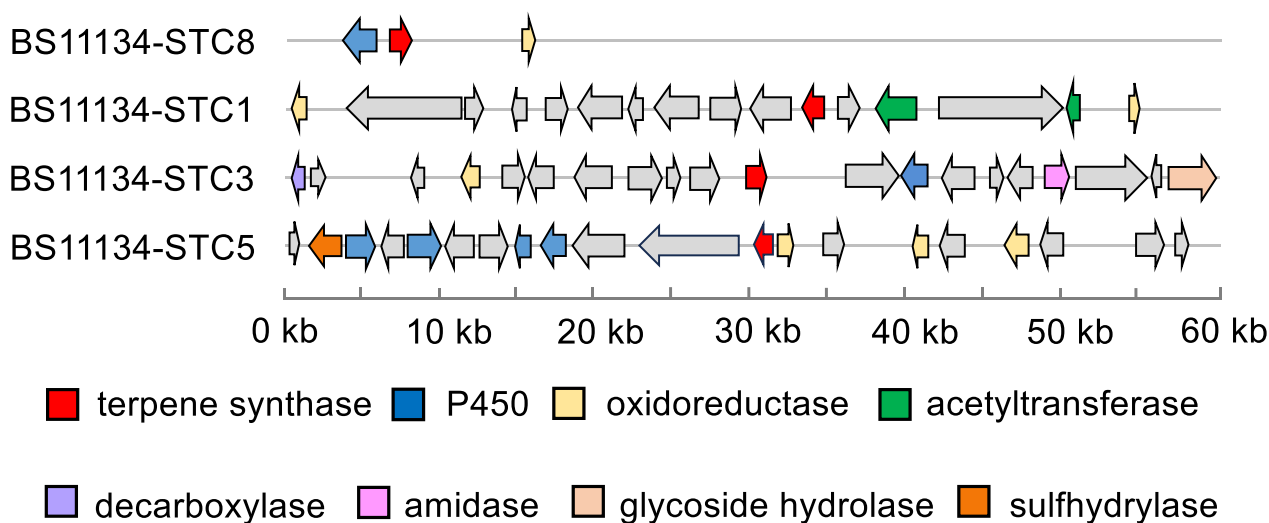


Fig. 1 Organization of the sesquiterpenoids biosynthetic gene cluster in BS11134

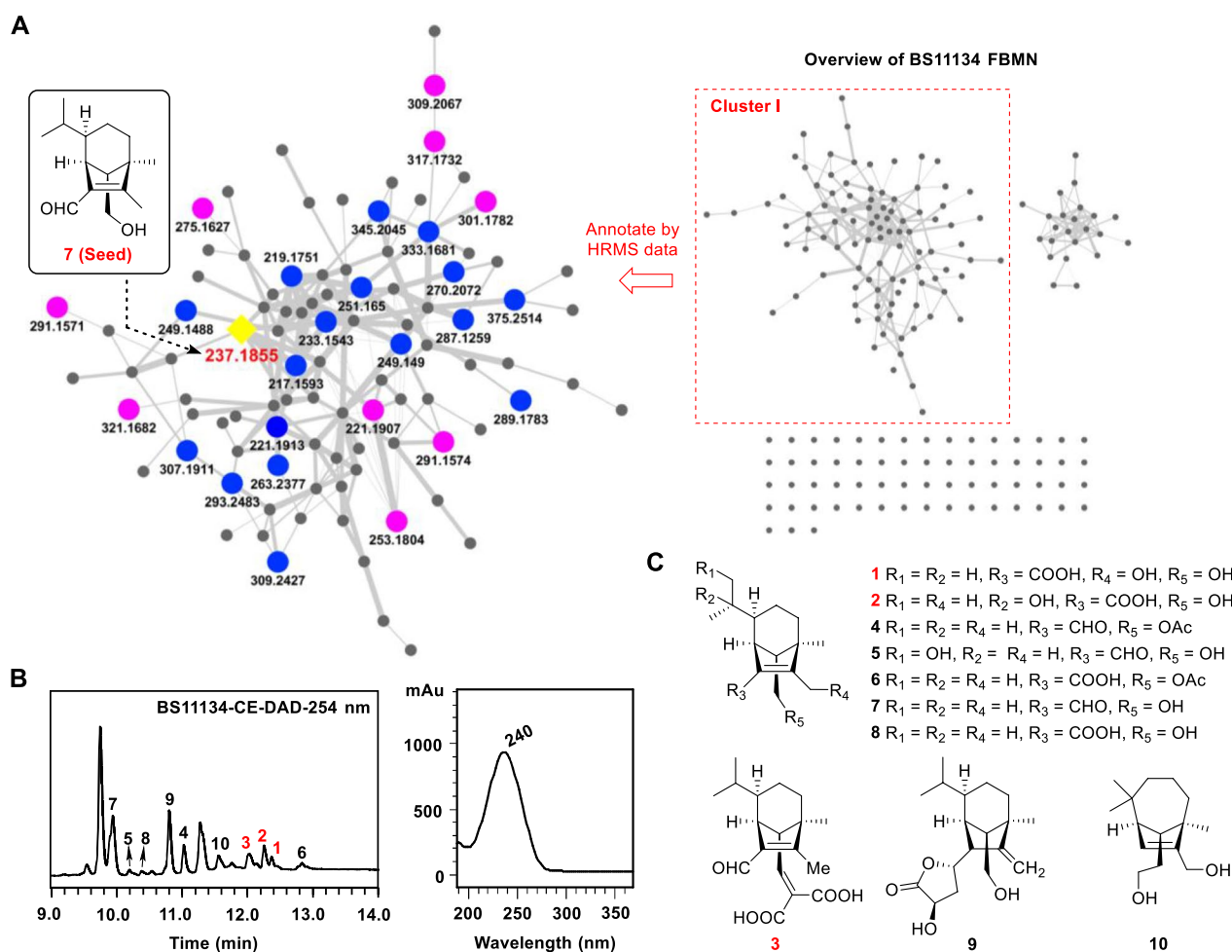


Fig. 2 FBMN-guided characterization of new helminthosporol analogs from BS11134 crude extract. **A** Clustering of sesquiterpenoids analogs. Helminthosporol (**7**) was used as seed compound (yellow shaded square) in cluster analysis, and 26 analogs (Purple circles: compounds isolated in this study; Blue circles: other potential new sesquiterpenoids identified by HRMS annotation) were identified within the network. **B** HPLC–UV chromatogram of sesquiterpenoids fraction RD3 examined at 254 nm, and the UV spectrum of helminthosporol. **C** Structures of compounds **1–10** isolated from strain BS11134

with H-13, and H-13 coupled with H₂–14 (Fig. 3 and Table S1). The two hydroxyl groups at C-12 (δ_C 55.6) and C-14 (δ_C 59.9) could be further determined by the HMBC (Fig. S1f) correlations of oxymethine protons at δ_H 4.54 (d, $J = 13.2$ Hz) and 4.12 (d, $J = 13.2$ Hz) with C-1 (δ_C 128.5), C-2 (δ_C 157.7) and C-3 (δ_C 49.2), and oxymethine protons at δ_H 3.44 (dd, $J = 10.3, 4.9$ Hz), and 3.05 (dd, $J = 10.3, 9.4$ Hz) with C-3, C-7 (δ_C 43.2) and C-13 (δ_C 62.0). A six-membered ring was formed on C-13 was connected to C-4 through C-3, according to the HMBC correlations between H₃–8 and C-3, C-4, and C-13. The presence of a methyl group (Me-8) at C-3 was inferred as well. The olefinic carbons C-1 and C-2 were connected to C-7 and C-3, respectively, according to the HMBC correlations of H-7/C-15,

H-7/C-1, H-7/C-2, H₂–12/C-2, and H₂–12/C-3. These observations suggested the structure of compound **1** closely resembled helminthosporic acid [27], with the notable substitution of a methyl group for a hydroxyl-methylene group. The relative configurations of **1** could be established according to the ROESY (Fig. S1g) correlations of H-7/H₃–11, H-7/H-13, H₃–8/H-13, and H-13/H-6, as well as comparison with literature [27] (Fig. 3). To figure out the absolute configurations of **1**, the electronic circular dichroism (ECD) calculation of two epimers 3*R*,6*R*,7*S*,13*S*–**1**/3*S*,6*S*,7*R*,13*R*–**1** was performed, resulting in the 3*R*,6*R*,7*S*,13*S* configurations of **1** (Fig. 4A). Therefore, the structure of **1** was established (Fig. 2C) and it was named 12-hydroxyhelminthosporic acid.

Table 1 Detailed annotation for sesquiterpene related nodes in cluster I from the BS11134 featured based molecular networking

Node (observed precursor <i>m/z</i>)	Molecular formula	Calc. <i>m/z</i>	^a Δ (ppm)	Δ _{<i>m/z</i>}	Annotation
217.1593	C ₁₅ H ₂₁ O	217.1587	2.8	− 4.0320 from 10	− H ₄ from 10
219.1751	C ₁₅ H ₂₃ O	219.1743	3.7	− 2.0156 from 10	− H ₂ from 10
221.1907	C ₁₅ H ₂₅ O	221.1900	3.2	− 15.9948 from 7	Secolongifolene diol (10) [M−H ₂ O+H] ⁺
221.1913	C ₁₅ H ₂₅ O	221.1900	5.8	− 15.9942 from 7	Isomer of 10
233.1543	C ₁₅ H ₂₁ O ₂	233.1536	3.0	− 4.0312 from 10	− H ₄ from 7
237.1855	C ₁₅ H ₂₅ O ₂	237.1849	2.5	0.0000	Helminthosporol (7) [M+H] ⁺
249.1488	C ₁₅ H ₂₁ O ₃	249.1485	1.2	− 4.0316 from 5	− H ₄ from 5
249.149	C ₁₅ H ₂₁ O ₃	249.1485	2.0	− 4.0314 from 5	− H ₄ from 5
251.165	C ₁₅ H ₂₃ O ₃	251.1642	3.2	− 2.0154 from 5	− H ₂ from 5
253.1804	C ₁₅ H ₂₅ O ₃	253.1798	2.4	15.9949 from 7	5 [M+H] ⁺
263.2377	C ₁₈ H ₃₁ O	263.2369	3.0	42.047 from 6	+ C ₃ H ₆ from 6
270.2072	C ₁₅ H ₂₈ NO ₃	270.2064	3.0	17.0268 from 5	5 [M+NH ₄] ⁺
275.1627	C ₁₅ H ₂₄ O ₃ Na	275.1623	1.5	37.9772 from 7	Helminthosporic acid (8) [M+Na] ⁺
287.1259	C ₁₅ H ₂₀ O ₄ Na	287.1259	0.0	− 4.0312 from 1	− H ₄ from 1
289.1783	C ₁₆ H ₂₆ O ₃ Na	289.178	1.0	14.0156 from 8	+ CH ₂ from 8
291.1571	C ₁₅ H ₂₄ O ₄ Na	291.1572	0.3	15.9944 from 8	1 [M+Na] ⁺
291.1574	C ₁₅ H ₂₄ O ₄ Na	291.1572	0.7	15.9947 from 8	2 [M+Na] ⁺
293.2483	C ₁₉ H ₃₃ O ₂	293.2475	2.7	56.0628 from 7	+ C ₄ H ₈ from 7
301.1782	C ₁₇ H ₂₆ O ₃ Na	301.178	0.7	26.0155 from 8	4 [M+Na] ⁺
307.1911	C ₁₈ H ₂₇ O ₄	307.1904	2.3	− 2.0156 from 9	− H ₂ from 9
309.2067	C ₁₈ H ₂₉ O ₄	309.206	2.3	72.0212 from 7	Sorokinianin (9) [M+H] ⁺
309.2427	C ₁₉ H ₃₃ O ₃	309.2424	1.0	56.0623 from 5	+ C ₄ H ₈ from 5
317.1732	C ₁₇ H ₂₆ O ₄ Na	317.1729	0.9	42.0105 from 8	6 [M+Na] ⁺
321.1682	C ₁₈ H ₂₅ O ₅	321.1697	4.7	11.9615 from 9	3 [M+H] ⁺
333.1681	C ₁₇ H ₂₆ O ₅ Na	333.1678	0.9	15.9949 from 6	+ O from 6
345.2045	C ₁₉ H ₃₀ O ₄ Na	345.2042	0.9	28.0313 from 6	+ C ₂ H ₄ from 6
375.2514	C ₂₁ H ₃₆ NO ₄	375.2511	0.8	84.0943 from 1	+ C ₆ H ₁₂ from 1

^a Δ = (Observed *m/z* − Calc. *m/z*)/Calc. *m/z*

Compound **2** has a molecular formula of C₁₅H₂₄O₄, as confirmed by HRESIMS data (Fig. S2a). Comparative analysis of ¹H and ¹³C NMR data (Table 2 and Fig. S2b–d) between compounds **1** and **2** revealed that two secondary methyl groups [δ_C/δ_H 20.8/0.76 (d, *J* = 6.3 Hz), δ_C/δ_H 21.8/0.97 (d, *J* = 6.3 Hz)] were replaced by two methyl groups at lower field [δ_C/δ_H 28.0/1.13 (s), δ_C/δ_H 28.5/1.04 (s)]. The appearance of an oxygenated quaternary carbon (δ_C 70.5) suggested the presence of one hydroxyl group at C-9. HMBC (Fig. 3 and Supplementary Fig. S2e, f) further confirmed this hypothesis with correlations of H₃–10/C-6, H₃–10/C-9, H₃–10/C-11. Resonances at δ_H 1.88 (s) showed correlations with carbons at δ_C 49.5 (C-3), δ_C 127.6 (C-1), and δ_C 156.1 (C-2), establishing the methyl group location of C-12. The relative configurations of **2** were consistent with those of **1** by detailed analysis of their ROESY (correlations of H-7/H₃–11, H-7/H-13, H₃–8/H-13, and H-13/H-6) (Fig. 3, Fig. S2 g, and Table S2). The absolute configurations were

assigned as 3*R*,6*S*,7*R*,13*S* through ECD calculation. Thus, the structure of **2** was established (Fig. 2C), and this compound was named 9-hydroxyhelminthosporic acid.

The molecular formula of compound **3** was deduced as C₁₈H₂₄O₅ based on HRESIMS (Fig. S3a) (*m/z* 343.1514 [M+Na]⁺, calcd. for 343.1516) with 7 degrees of unsaturation. ¹H, ¹³C and 2D NMR data (Figs. S3b–f) revealed a similar structural skeleton with compound **1**, except for resonances of two additional carboxyls (δ_C 164.9, 166.8) and one olefinic bond (δ_C 145.6, 131.2). HMBC correlations from H-14 (δ_H 6.51 d, *J* = 10.9 Hz) to C-3, C-7, C-16, C17, and C-18 revealed that two carboxyl groups were connected with C-14 through non-protonated carbon C-16. The relative configurations of **3** were consistent with **1** based on key ROESY correlations of H-7/H₃–11, H-7/H-13, H₃–8/H-13, and H-13/H-6 (Fig. 3, Fig. S3 g, and Table S3). Given the shared biosynthetic pathway of compounds **1** and **3** through the *seco*-sativene

Table 2 ¹H and ¹³C NMR Data of compounds **1–5**

Pos	1 ^a		2 ^b		3 ^c		4 ^c		5 ^a	
	δ _C , mult	δ _H , mult (J in Hz)	δ _C , mult	δ _H , mult (J in Hz)	δ _C , mult	δ _H , mult (J in Hz)	δ _C , mult	δ _H , mult (J in Hz)	δ _C , mult	δ _H , mult (J in Hz)
1	128.5, C		127.9, C		136.2, C		136.0, C		137.1, C	
2	157.7, C		156.1, C		165.7, C		166.0, C		168.7, C	
3	49.2, C		49.5, C		51.8, C		50.4, C		50.8, C	
4	34.9, CH ₂	1.48, m	33.1, CH ₂	1.33, m	32.6, CH ₂	1.50, m	33.1, CH ₂	1.39, m	34.3, CH ₂	1.43, m
5a	24.8, CH ₂	1.26, m		1.28, m		1.30, m		1.66, m		1.73, m
5b		1.64, m	20.4, CH ₂	1.59, m	24.6, CH ₂	1.70, m	24.7, CH ₂	1.66, m	25.4, CH ₂	1.73, m
6	44.8, CH	0.97, m		1.28, m		0.85, m		0.81, m		0.90, m
7	43.2, CH	3.09, brs	48.4, CH	1.30, m	43.7, CH	1.00, m	44.1, CH	0.98, m	40.3, CH	1.43, m
8	18.7, CH ₃	0.99, s	41.7, CH	3.06, brs	44.4, CH	2.83, brs	41.0, CH	2.94, brs	41.4, CH	3.39, brs
9	31.4, CH	1.16, m	18.9, CH ₃	0.88, s	18.9, CH ₃	0.93, s	18.0, CH ₃	1.00, s	18.4, CH ₃	1.02, s
10	21.8, CH ₃	0.97, d (6.3)	70.5, C		31.0, CH	0.94, m	31.1, CH	0.94, m	39.2, CH	1.11, m
11	20.8, CH ₃	0.76, d (6.3)	28.5, CH ₃	1.04, s	21.5, CH ₃	0.97, d (6.0)	21.5, CH ₃	0.99, d (6.3)	15.8, CH ₃	0.80, d (6.9)
12	55.6, CH ₂	4.54, d (13.2)	28.0, CH ₃	1.13, s	20.5, CH ₃	0.73, d (6.0)	20.5, CH ₃	0.73, d (6.5)	67.7, CH ₂	3.87, dd (11.1, 3.9)
13	62.0, CH	4.12, d (13.2)		1.88, s		2.08, s		2.03, s		3.62, dd (11.1, 4.7)
14	59.9, CH ₂	1.42, dd (9.4, 4.9)	12.2, CH ₃	1.50, dd (9.5, 5.2)	10.5, CH ₃		10.3, CH ₃		10.9, CH ₃	2.03, s
15	167.5, C	3.44, dd (10.3, 4.9)	63.3, CH	3.40, dd (10.2, 5.2)	59.6, CH	2.42, d (10.9)	56.9, CH	1.75, dd (9.0, 5.5)	61.0, CH	1.73, dd (9.9, 4.7)
16		3.05, dd (10.3, 9.4)	59.8, CH ₂	3.06, dd (10.2, 9.5)	145.6, CH	6.51, d (10.9)	63.6, CH ₂	4.00, dd (11.1, 5.5)	61.8, CH ₂	3.62, dd (11.1, 4.7)
17					188.6, CH	10.03, s	188.4, CH	9.99, s	189.4, CH	3.26, dd (11.1, 9.9)
18			168.7, C		131.2, C		170.4, C			10.00, s
					164.9, C		20.7, CH ₃	1.98, s		
					166.8, C					

^a Recorded in CDCl₃, ¹H 500 MHz; ¹³C 125 MHz; ^b Recorded in DMSO-*d*₆, ¹H 500 MHz; ¹³C 125 MHz; ^c Recorded in DMSO-*d*₆, ¹H 800 MHz; ¹³C 200 MHz

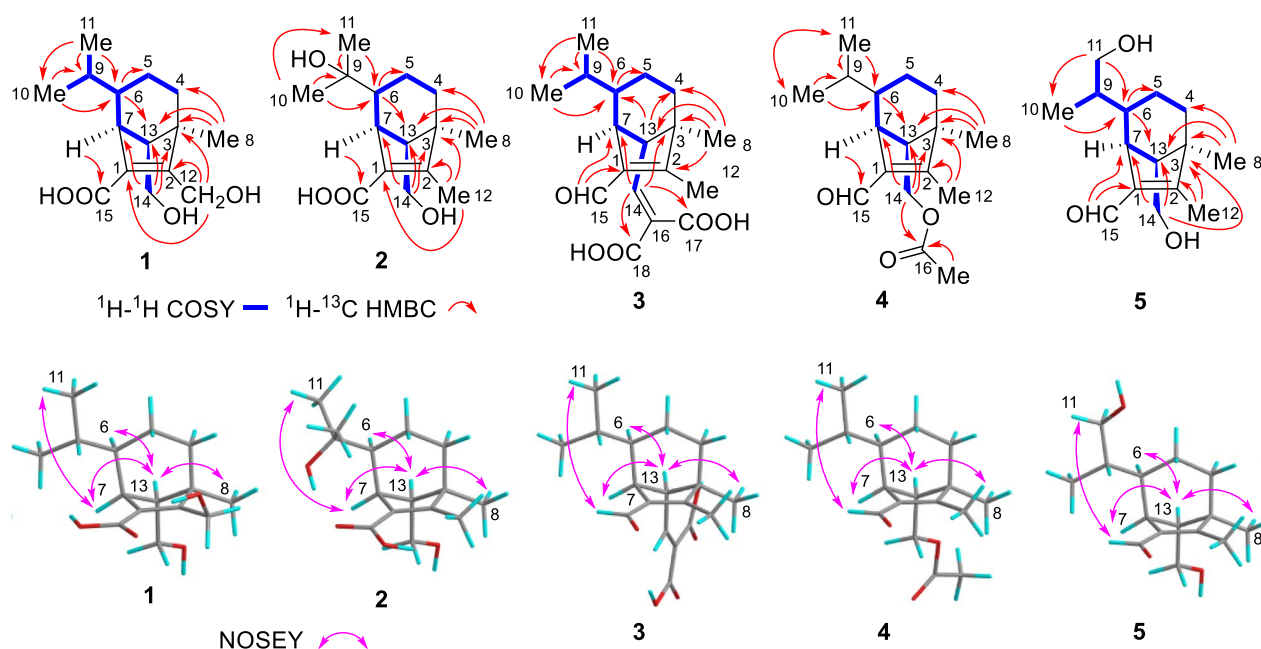


Fig. 3 2D NMR correlations of compounds 1–5. **A** Key ^1H - ^1H COSY and ^1H - ^{13}C HMBC correlations. **B** Key ROESY correlations

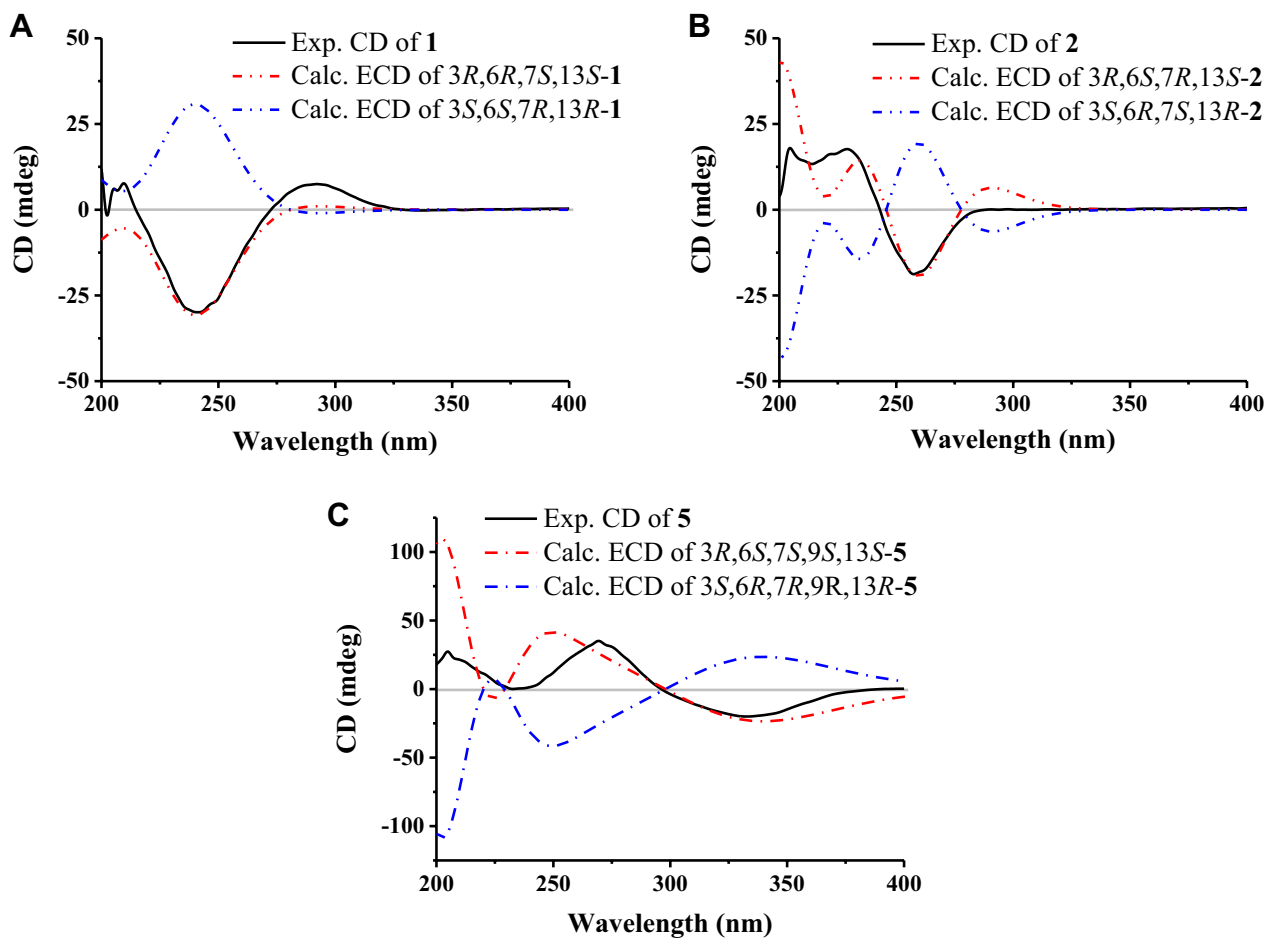


Fig. 4 Experimental and computed ECD of compounds 1 (A), 2 (B), and 5 (C)

sesquiterpene skeleton, the absolute configurations of **3** were deduced to align with that of **1**, and was designated 3*R*,6*R*,7*S*,13*S*. This alignment was supported by its specific optical rotation ($[\alpha]_{\text{D}} -20$) in contrast to compound **1** ($[\alpha]_{\text{D}} -38$) and to bipolarisorokin H ($[\alpha]_{\text{D}} -137$) [28]. Thus, **3** was a new compound (Fig. 2C) and named bipolarisorokin I.

HRESIMS of **4** displayed a molecular ion peak at m/z 301.1775 for $[M+Na]^+$ (calcd. for 301.1774) (Fig. S4a) and indicating a molecular formula of $C_{17}H_{26}O_3$. 1D and 2D NMR data (Figs. S4b–f) showed that compound **4** shared a structural framework with helminthosporol (**7**) [29], distinguished by an additional acetyl group [δ_C/δ_H 20.7/1.98 (s), δ_C 170.4]. HMBC correlations from H_3-17 and H_2-14 to C-16 confirmed compound **4** as a 14-OH acetylated analogue of **7**. Through ROESY analysis, the crosspeaks of H-7/ H_3-11 , H-7/H-13, H_3-8 /H-13, and H-13/H-6 revealed that the relative configurations of **4** were consistent with those of **1** (Fig. 3, Fig. S4 g, and Table S4). Its absolute configurations were deduced as 3*R*,6*R*,7*S*,13*S* considering its biosynthetic lineage from *seco*-sativene sesquiterpene, and comparison of specific rotation values (**4**, $[\alpha]_{\text{D}} +11.0$) with literature (bipolenin H, $[\alpha]_{\text{D}} +17.5$) [30]. Accordingly, compound **4** was definitively identified and named bipolarisorokin J, with a defined structure (Fig. 2C). The NMR data of compound **4** is reported here for the first time.

Compound **5** possessed a molecular formula of $C_{15}H_{24}O_3$ (four degrees of unsaturation) determined by HRESIMS data (Fig S5a). NMR analysis (1H and ^{13}C , Table 2 and Figs. S5b–S5 d) revealed a structural resemblance to helminthosporol (**7**), except that the methyl group (Me-11) was replaced by a hydroxyl-methylene group. The presence of a hydroxyl group at C-11 could be assigned by HMBC (Fig. 3 and Fig. S5e, f) correlations of the downfield shifted signals at δ_H 3.87 (dd, $J = 11.1, 3.9$ Hz) and 3.62 (dd, $J = 11.1, 4.7$ Hz) with C-6, C-9 and C-10. Detailed analysis of ROESY afforded the 3*R**,6*S**,7*S**,13*S** relative configuration in **5** (Fig. 4B, Fig. S5 g, Table S5). The relative configurations between C-6 and C-9 in **5** was determined to be 6*S**,9*S** by ^{13}C NMR calculations and DP4+ analyses (Fig. 5, Table S9) [31]. ECD calculations confirmed the absolute configurations of **5** as 3*R*,6*S*,7*S*,9*S*,13*S*, leading to the identification of compound **5** as 11-hydroxy-helminthosporol (Fig. 2) [32].

Compounds **6–10** were identified as helminthosporic acid derivative (**6**) [33], helminthosporol (**7**) [29], helminthosporic acid (**8**) [27], sorokinianin (**9**) [34], and secolongifolene diol (**10**) [29], by comparing their spectroscopic data with those in previous literature.

2.4 Proposed biosynthetic pathway of the isolated sesquiterpenoids

Sativene could be synthesized from FPP by sesquiterpene synthase (Fig. 6), by a mechanism involving ionization and successive rearrangement [35]. Compounds **1–9** belong to *seco*-sativene type irregular terpenoids, while compound **10** belongs to *seco*-longifolene type sesquiterpenoids [29]. The plausible biosynthetic routes of compounds **1–10** were described based on recent research [26, 36] (Fig. 6).

Intermediate **IM2** was generated from sativene through successive oxidation by P450 and a spontaneous shift of the $\Delta^{2,12}$ olefinic bond. Subsequent reduction of the C-14 aldehyde, catalysed by a Aldo-keto reductase (AKR) yielded compound **7**. Compounds **4**, **5**, and **8** can be derived from Compound **7** through acetylation at 14-OH, hydroxylation at C-11, and carboxylation of C-15, respectively. Hydroxylation at C-9 or C-12 of compound **8** yielded compounds **1** and **2**, respectively. Compound **6** resulted from the acetylation at 14-OH of Compound **8**. The γ -butyrolactone moiety in Compound **9** was proposed to derive from the TCA cycle intermediate 2-oxosuccinic acid via an aldol condensation reaction, as supported by previous isotope labelling studies [37]. A similar process occurred with compound **3**, where the 2-methylenemalonic acid moiety was incorporated using malonic acid as intermediate through an aldol condensation reaction with C-14 aldehyde of **IM2** (Fig. 6B). *seco*-Longifolene type sesquiterpenoid **10** was postulated to possess a divergent cyclization route, generating an end product with a seven-membered ring [27, 38].

2.5 In vitro anti-inflammatory assay

All isolated sesquiterpenoids from strain BS11134 were screened for their anti-inflammatory activity (Table 3) by evaluating inhibition effects on the NO production induced by LPS in RAW264.7, a mouse macrophage cell line. Compounds **1** and **9** exhibited anti-inflammatory effects in vitro, with inflammation inhibition rates of $28.0 \pm 2.4\%$ and $84.7 \pm 1.7\%$, respectively, at a concentration of 10 μM , compared to the positive control, indomethacin, which showed a $51.2 \pm 8.2\%$ inhibition rate.

3 Discussion and conclusion

The fungal kingdom is a primary source of new natural products, yet the capabilities of only a few species have been uncovered [39]. Terpenoids represent a crucial class of natural products derived from filamentous fungi. Fungal sesquiterpenoids, in particular, are significant targets for medical drug design because of their potential bioactivity [14, 40]. Our research uncovered ten sesquiterpenoids with a sativene architecture from the phytopathogenic fungus *B. sorokiniana* 11134.

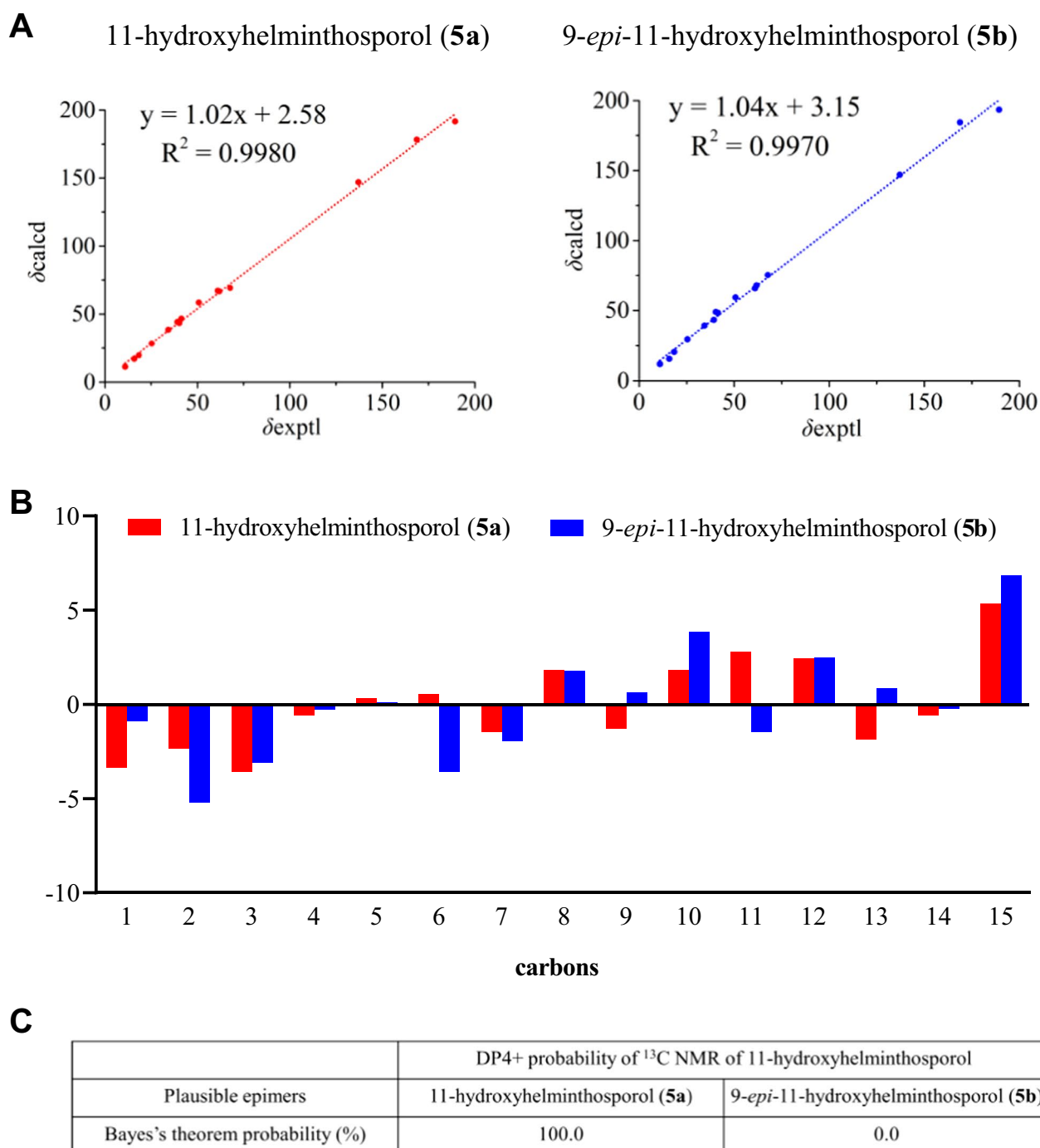


Fig. 5 ^{13}C NMR calculation results of two plausible isomers **5a/5b** at the B3LYP/6–311++G(2 d,p) level. **A** Linear correlation plots of the calculated and experimental ^{13}C NMR values. **B** Relative errors between the calculated and recorded ^{13}C values. **C** DP4+ probability

Several structural classes related to our isolated compounds have been previously reported from related members of the family Pleosporaceae including species of *Bipolaris*, *Cochliobolus*, and *Drechslera*; such compounds include sativene, *seco*-sativene, isosativene, longifolene,

and *seco*-longifolene. We expand the reported *seco*-sativene repertoire with three new congeners **1–3**. *seco*-sativenes sesquiterpenoids, characterized by a bicyclo[3.2.1]octane structure (6–5 ring system) [41], are biosynthetically generated from sativene through the

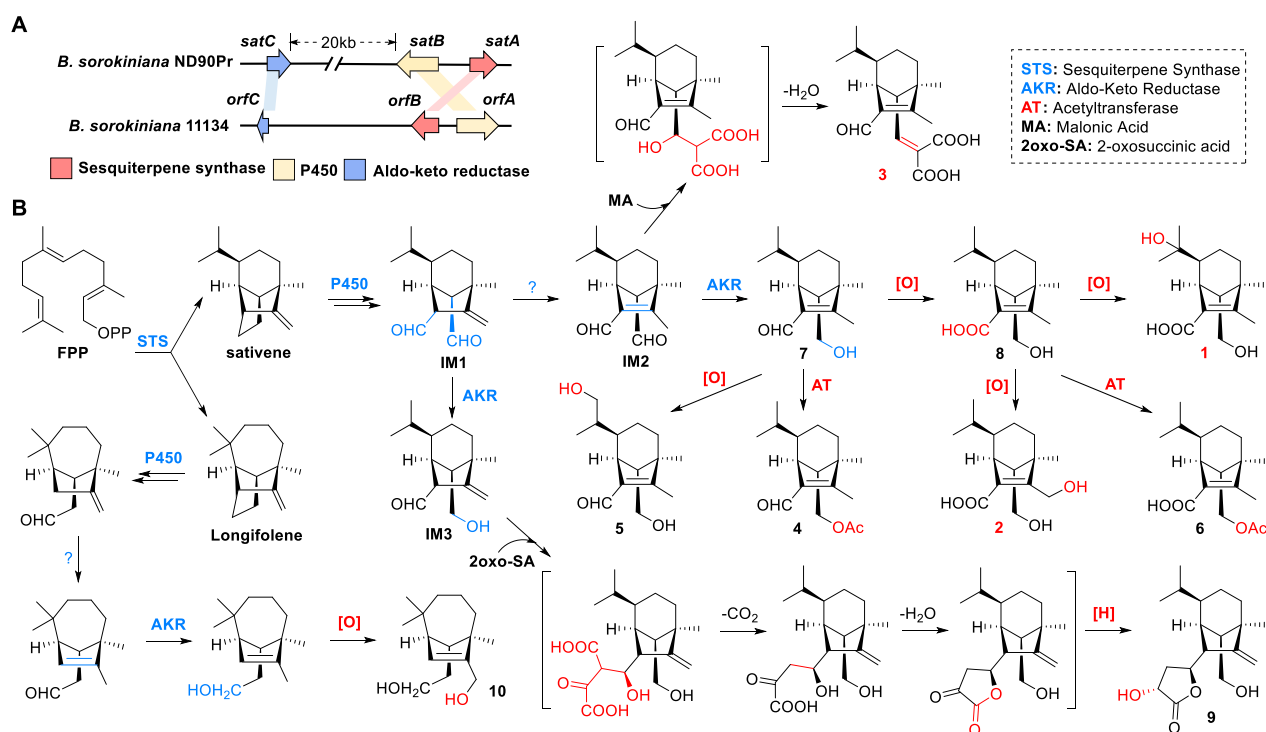


Fig. 6 Organization of the *seco*-sativene biosynthetic gene cluster in *B. sorokiniana* ND90Pr and BS11134 (**A**), and proposed biosynthetic pathway for isolated sesquiterpenoids **1–10** (**B**)

C14–C15 bond cleavage, and undergo various post-modifications such as isomerization, ketone reduction, acetylation, carboxylation, and glycosylation [41].

Recently, Zhang et al. revealed the biosynthetic gene cluster of *seco*-sativenes in *B. sorokiniana* ND90Pr through heterologous expression of a three-gene cassette in *Aspergillus nidulans*. The terpene cyclase (SatA) responsible for forming the 6-5-5 ring sativene skeleton, the cytochrome P450 (SatB) involved in C14–C15 bond cleavage, and the aldo–keto reductase (SatC) for the regioselective reduction of C14 aldehyde have been characterized [26]. We detected a similar three-gene cassette in strain BS11134, responsible for the biosynthesis of compounds **1–10**, showing high similarity to the *sat* cluster

(Fig. 6A). The proposed biosynthetic pathway for compounds **1–10** suggested that additional, yet unidentified enzymes (acetylase, oxidoreductase, double-bond translocase, etc.) are required for transforming the key intermediate **IM1** into these sesquiterpenoids (Fig. 6B).

Currently, more than 40 *seco*-sativenes featuring the bicyclo[3.2.1]octane structure have been isolated from fungi, exhibiting diverse bioactivities such as phytotoxicity, growth promotion, anti-NO production, ACAT inhibition, and antifungal effects [41]. In this study, we reported the NO production inhibition activity of sorokinianin ($84.7 \pm 1.7\%$ at $10 \mu\text{M}$) for the first time, which has been recognized as phytotoxin for decades [34]. Previously, only a few *seco*-sativene sesquiterpenoids were known for their anti-inflammatory potential. For instance, bipolenins G and 9-hydroxyhelminthosporol demonstrated anti-NO production activities with IC_{50} values of 23.8 and $17.5 \mu\text{M}$, respectively [30].

In summary, feature-based molecular networking generated from GNPS confirmed the cluster of sesquiterpenoids, and HRMS-oriented isolation led to the characterization of ten sesquiterpenoids with a helminthoporene skeleton, including three new compounds (**1–3**), alongside the first detailed NMR data for compound **4**. The structures of these compounds were unequivocally determined through comprehensive analyses

Table 3 NO inhibitory activities of compounds

Compound	% NO inhibition ($10 \mu\text{M}$)
1	28.0 ± 2.4
2	10.9 ± 2.3
8	14.4 ± 2.5
9	84.7 ± 1.7
Indomethacin	51.2 ± 2.0

of MS and NMR data. This research extends the known helminthoporene class of molecules and underscores the untapped potential of phytopathogenic fungi as sources of novel compounds.

4 Materials and methods

4.1 General experimental section

NMR spectra were recorded using a Bruker Advance DRX600 spectrometer and Bruker Advance III HDX 800 MHz spectrometer. Deuterated solvents (CDCl_3 and $\text{DMSO}-d_6$) were purchased from Cambridge Isotope Laboratories (CIL). A Bruker Maxis II ETD QTOF mass spectrometer was used to run HRESIMS analysis. Column chromatography was performed with Sephadex LH-20 (GE Healthcare BioSciences AB) and ODS-A (YMC, Japan). Semi-preparative HPLC was carried out equipped with Phenomenex Luna C18 (5 μm , 9.4×250 mm), Eclipse XDB-C3 (5 μm , 9.4×250 mm), and ZORBAX RX-C8 (9.4 $\times 250$ mm) columns. HPLC analysis were carried out with an Agilent 1100 Series separation module coupled with DAD detector. The UV-vis spectra were measured using a Cary 50 spectrophotometer. The optical rotation was recorded on a Perkin-Elmer Model 343 polarimeter. Biological media, reagents, and chemicals were obtained from standard commercial sources.

4.2 Characterization and identification of pathogenic fungus BS11134

The original culture of BS11134 was obtained from a leaf of *Poa pratensis* collected from Sujiatun (GPS 40.21432, 116.53574), Chaoyang District, Beijing, in July 2013. It was characterized as *Bipolaris sorokiniana* by ITS DNA gene sequence (accession no. KU297882) and morphology [42], and has been deposited in the China General Microbiological Culture Collection Center (accession No. 3.18317), which is a member of the World Data Centre for Microorganisms (WDCM 550).

4.3 GNPS directed dereplication and prediction of new sesquiterpenoids

Samples were dissolved in MeOH to make 1 mg/mL solution and eluted with a gradient of H_2O (1% HCOOH) and CH_3CN with a gradient method as follows: 5% CH_3CN gradient elution to 99% in 9 min, 99% CH_3CN kept for 3 min, 99% CH_3CN changed to 5% in 0.1 min, and 5% CH_3CN kept for 3 min with the flow rate of 0.35 mL/min. LC-MS/MS data was acquired on Bruker Maxis II ETD QTOF mass spectrometer coupled with Thermo scientific UltiMate 3000 HPLC system. The raw data was converted to the mzXML file format using the Bruker Data Analysis software. The mzML file was processed using the MZmine (version 2.53). The mass detections were realized keeping the noise level at 1.0E^3 for MS1 and

1.0E^1 for MS2, respectively. The ADAP chromatogram building used a minimum time span of 0.1 min, m/z tolerance of 0.02 (or 5 ppm), and minimum height of 1.0E^3 . Deisotop was carried out utilizing isotopic peaks grouper algorithm, with a RT tolerance of 0.1 min and m/z tolerance of 0.001 (or 5 ppm). Duplicate peaks were filtered with filter mode of old average, m/z tolerance of 0.001 (or 5 ppm), and retention time (RT) range = 1 min. A feature-based molecular networking was created using the web-based workflow (version release_28.2) at GNPS (<https://gnps.ucsd.edu/>) [17, 19]. Cytoscape (version 3.7.2) was used to visualize the corresponding output FBMN data.

4.4 Scale-up fermentation and secondary metabolites purification

The strain BS11134 was cultured on potato dextrose agar (PDA) at 28 °C for 10 days. The well-grown agar cultures were cut into small cubes ($0.5 \times 0.5 \times 0.5 \text{ cm}^3$) and used to inoculate 250 mL Erlenmeyer flasks containing 50 mL PDB medium, which were further incubated on a rotary shaker at 28 °C, 170 rpm for 5 days to generate the seed culture. The scale-up fermentation was carried out with twenty 1000 mL Erlenmeyer flasks, each containing 160 g of rice and 240 mL of distilled water, soaked overnight, followed by being autoclaved at 15 psi for 30 min. Then each flask was inoculated with 12 mL of the seed culture, and grown at 28 °C for 40 days.

The fermentation products were extracted exhaustively with EtOAc and were concentrated in vacuo. The crude extracts (27.7 g) were separated by silica gel, Sephadex LH-20 column chromatography and ODS-MPLC [43], to obtain sub-fractions containing the sesquiterpenoids, guided by the molecular networking and LC-MS results. Among these sub-fractions, E1 C7D (89 mg) was further separated by preparative-HPLC running with Eclipse XDB-C8 (9.4 $\times 250$ mm) column at a flow rate of 3.0 mL/min eluting with the following gradient: 0 min, 50% $\text{CH}_3\text{CN}-\text{H}_2\text{O}$; 30 min 50% CH_3CN ; 60 min 70% CH_3CN to obtain 7 (1.5 mg, $t_R = 13.9$ min). E6B was separated by ODS-MPLC using gradient elution from 50 to 100% $\text{CH}_3\text{OH}-\text{H}_2\text{O}$ for 170 min to obtain eleven fractions (E6B1-E6B11). E6B9 was purified on a Sephadex LH-20 column using CH_3OH to obtain compound 4 (1.0 mg). E6B7-2 (100 mg) was purified by preparative RP-HPLC using an Eclipse XDB-C8 (9.4 $\times 250$ mm) column eluting at a flow rate of 3.0 mL/min using a gradient elution: 0 min, 20% $\text{CH}_3\text{CN}-\text{H}_2\text{O}$; 30 min 20% $\text{CH}_3\text{CN}-\text{H}_2\text{O}$; 42 min 23% $\text{CH}_3\text{CN}-\text{H}_2\text{O}$ to obtain 1 (9.5 mg, $t_R = 40.1$ min). E6B7-10 (145 mg) was purified by preparative RP-HPLC using a ZORBAX RX-C8 (9.4 $\times 250$ mm) column eluting at a flow rate of 3.0 mL/min using a gradient elution: 0 min, 25% $\text{CH}_3\text{CN}-\text{H}_2\text{O}$; 26 min 34% $\text{CH}_3\text{CN}-\text{H}_2\text{O}$ to obtain 2 (22.0 mg, $t_R = 21.4$ min). E6B7-8 (142 mg)

was purified by preparative RP-HPLC using an ZORBAX RX-C8 (9.4 × 250 mm) column eluting at a flow rate of 3.0 mL/min using a gradient elution: 0 min, 20% CH₃CN–H₂O; 24 min 36% CH₃CN–H₂O to obtain **3** (26.2 mg, t_R = 16.6 min). E2 C6 (470 mg) was purified by preparative RP-HPLC using an Phenomenex Luna C18 column (5 μm, 9.4 × 250 mm) eluting at a flow rate of 4.0 mL/min using a gradient elution: 0 min, 60% CH₃OH–H₂O; 25 min 95% CH₃OH–H₂O to obtain **5** (1.0 mg, t_R = 18.3 min). E2D3 (349 mg) was purified by preparative RP-HPLC using an Eclipse XDB-C3 column (5 μm, 9.4 × 250 mm) eluting at a flow rate of 3.0 mL/min using a gradient elution: 0 min, 40% CH₃CN–H₂O; 25 min 60% CH₃OH–H₂O to obtain **6** (2.1 mg, t_R = 21.3 min). Fraction E3 was fractionated on a Sephadex LH-20 column using CH₂Cl₂–CH₃OH (1:1) to give 33 fractions (1–33). Sub-fraction E3–24 (150 mg) was purified by preparative RP-HPLC using an ZORBAX RX-C8 (9.4 × 250 mm) column eluting at a flow rate of 3.0 mL/min using a gradient elution: 0 min, 35% CH₃CN–H₂O; 50 min 45% CH₃CN–H₂O to obtain **8** (9.9 mg, t_R = 30.1 min) and **9** (4.4 mg, t_R = 40.0 min). E3D4 (190 mg) was purified by preparative RP-HPLC using an Phenomenex Luna C18 column (5 μm, 9.4 × 250 mm) eluting at a flow rate of 4.0 mL/min using a gradient elution: 0 min, 50% CH₃OH–H₂O; 25 min 80% CH₃OH–H₂O to obtain **10** (2.2 mg, t_R = 20.0 min).

4.5 Quantum chemical computation details of ECD and ¹³C NMR spectra

Calculations were performed using the density functional theory (DFT) as carried out in Gaussian 03 [44], with the methods described in previous study [42, 45].

4.6 In vitro anti-inflammatory assay

The in vitro anti-inflammatory assay followed the methods of Yang et al. [46].

Supplementary Information

The online version contains supplementary material available at <https://doi.org/10.1007/s13659-025-00508-9>.

Supplementary Material 1

Acknowledgements

We are grateful for the funding support from the National Key Research and Development Program of China (2019YFA0906200 to X.L., and 2020YFA0907200 to J.Z.); the the Shanghai Sci-Tech Inno Center for Infection & Immunity (Grant No. SSIII-2024 A02 to G.Z.); the National Natural Science Foundation of China (31430002, 31720103901, and 32121005 to L.Z.; 21977029 to X.L.); Shanghai Rising-Star Program (20QA1402800) to J.Z.; the Open Project Funding of the State Key Laboratory of Bioreactor Engineering, the 111 Project (B18022); Shanghai Science and Technology Commission (18

JC1411900); and the Shandong Taishan Scholar Program of China to L.Z.; and the Natural Science and Engineering Research Council of Canada to T. H.

Author contributions

Lixin Zhang and Xueting Liu designed this study. Jingyu Zhang, Ronald J Quinn, Guoliang Zhu and Jianying Han arranged the research consortium. Qiang Yin, Jianying Han, Jingyu Zhang, Keke Zou, Kangjie Lv, Zexu Lin, Zhijun Song and Guixiang Yang performed fermentation, compound purification, and structural elucidation. Tom Hsiang sequenced and assembled genomic data and revised the manuscript. Lei Ma and Miaomiao Liu analyzed the biological data. Jianying Han, Jingyu Zhang, Guoliang Zhu and Xueting Liu drafted this manuscript. All authors read and approved the final manuscript.

Funding

This study was funded by National Key Research and Development Program of China (2019YFA0906200, 2020YFA0907200); National Natural Science Foundation of China (31430002, 31720103901, 32121005, 21977029); Shanghai Rising-Star Program (20QA1402800); Open Project Funding of the State Key Laboratory of Bioreactor Engineering (B18022); Shanghai Science and Technology Commission (18 JC1411900); Shanghai Sci-Tech Inno Center for Infection & Immunity (SSIII-2024 A02).

Availability of data and materials

Data will be made available on request.

Declarations

Competing interests

All authors declare no competing financial interests.

Author details

¹State Key Laboratory of Bioreactor Engineering, East China University of Science and Technology, Shanghai 200237, China. ²Griffith Institute for Drug Discovery, Griffith University, Brisbane, QLD, Australia. ³Institute for Molecular Bioscience, The University of Queensland, St. Lucia, QLD 4072, Australia. ⁴Chinese Academy of Sciences, Key Laboratory of Pathogenic Microbiology and Immunology, Institute of Microbiology, Chinese Academy of Sciences, Beijing, China. ⁵School of Environmental Sciences, University of Guelph, Guelph, ON N1G 2W1, Canada.

Received: 13 January 2025 Accepted: 27 March 2025

Published online: 09 May 2025

References

- Berenbaum F. Proinflammatory cytokines, prostaglandins, and the chondrocyte: mechanisms of intracellular activation. *Joint Bone Spine*. 2000;67(6):561–4. [https://doi.org/10.1016/S1297-319X\(00\)00212-8](https://doi.org/10.1016/S1297-319X(00)00212-8).
- Reddy DB, Reddanna P. Chebulagic acid (CA) attenuates LPS-induced inflammation by suppressing NF-κB and MAPK activation in RAW 264.7 macrophages. *Biochem Biophys Res Commun*. 2009;381(1):112–7. <https://doi.org/10.1016/j.bbrc.2009.02.022>.
- Salminen A, Ojala J, Kauppinen A, Kaarniranta K, Suuronen T. Inflammation in Alzheimer's disease: amyloid-β oligomers trigger innate immunity defence via pattern recognition receptors. *Prog Neurobiol*. 2009;87(3):181–94. <https://doi.org/10.1016/j.pneurobio.2009.01.001>.
- Shah IM, Macrae IM, Di Napoli M. Neuroinflammation and neuroprotective strategies in acute ischaemic stroke—from bench to bedside. *Curr Mol Med*. 2009;9(3):336–54. <https://doi.org/10.2174/156652409787847236>.
- J B. Dictionary of natural products on CD-ROM. Version 101; 2002.
- Hana B, Veronika H, Lenka S, Martin A, Iva B. Antioxidant, pro-oxidant and other biological activities of sesquiterpenes. *Curr Top Med Chem*. 2014;14(22):2478–94. <https://doi.org/10.2174/1568026614666141203120833>.
- Jesus Duran-Pena M, Botubol Ares JM, Hanson JR, Collado IG, Hernandez-Galan R. Biological activity of natural sesquiterpenoids containing a gem-dimethylcyclopropane unit. *Nat Prod Rep*. 2015;32(8):1236–48. <https://doi.org/10.1039/c5np00024f>.

8. Elissawy AM, El-Shazly M, Ebada SS, Singab AB, Proksch P. Bioactive terpenes from marine-derived fungi. *Mar Drugs*. 2015;13(4):1966–92. <https://doi.org/10.3390/md13041966>.
9. Gliszczynska A, Brodelius PE. Sesquiterpene coumarins. *Phytochem Rev*. 2012;11(1):77–96. <https://doi.org/10.1007/s11101-011-9220-6>.
10. Orofino Kreuger MR, Grootjans S, Biavatti MW, Vandenabeele P, Dherde K. Sesquiterpene lactones as drugs with multiple targets in cancer treatment: focus on parthenolide. *Anticancer Drugs*. 2012;23(9):883–96. <https://doi.org/10.1097/CAD.0b013e328356cad9>.
11. Spivey AC, Weston M, Woodhead S. Celastraceae sesquiterpenoids: biological activity and synthesis. *Chem Soc Rev*. 2002;31(1):43–59. <https://doi.org/10.1039/b000678p>.
12. Tanasova M, Sturla SJ. Chemistry and biology of acylfulvenes: sesquiterpene-derived antitumor agents. *Chem Rev*. 2012;112(6):3578–610. <https://doi.org/10.1021/cr2001367>.
13. Yang X-L, Zhang J-Z, Luo D-Q. The taxonomy, biology and chemistry of the fungal *Pestalotiopsis* genus. *Nat Prod Rep*. 2012;29(6):622–41. <https://doi.org/10.1039/c2np00073c>.
14. Abraham WR. Bioactive sesquiterpenes produced by fungi: are they useful for humans as well? *Curr Med Chem*. 2001;8(6):583–606. <https://doi.org/10.2174/0929867013373147>.
15. Kramer R, Abraham W-R. Volatile sesquiterpenes from fungi: what are they good for? *Phytochem Rev*. 2012;11(1):15–37. <https://doi.org/10.1007/s11101-011-9216-2>.
16. Quinn RA, Nothias L-F, Vining O, Meehan M, Esquenazi E, Dorrestein PC. Molecular networking as a drug discovery, drug metabolism, and precision medicine strategy. *Trends Pharmacol Sci*. 2017;38(2):143–54. <https://doi.org/10.1016/j.tips.2016.10.011>.
17. Wang M, Carver JJ, Phelan VV, Sanchez LM, Garg N, Peng Y, et al. Sharing and community curation of mass spectrometry data with Global Natural Products Social Molecular Networking. *Nat Biotechnol*. 2016;34(8):828–37. <https://doi.org/10.1038/nbt.3597>.
18. Watrous J, Roach P, Alexandrov T, Heath BS, Yang JY, Kersten RD, et al. Mass spectral molecular networking of living microbial colonies. *Proc Natl Acad Sci USA*. 2012;109(26):E1743–52. <https://doi.org/10.1073/pnas.1203689109>.
19. Nothias L-F, Petras D, Schmid R, Duehrkop K, Rainer J, Sarvepalli A, et al. Feature-based molecular networking in the GNPS analysis environment. *Nat Methods*. 2020;17(9):905. <https://doi.org/10.1038/s41592-020-0933-6>.
20. Mayo PD, Spencer EY, White RW. Helminthosporal, the toxin from *Helminthosporium sativum*. I. Isolation and characterization. *Can J Chem*. 1961;39(8):1608–12. <https://doi.org/10.1139/v61-205>.
21. Gayed SK. Production of symptoms of barley leaf-spot disease by culture filtrate of *Helminthosporium sativum*. *Nature*. 1961;191(4789):725–6. <https://doi.org/10.1038/191725b0>.
22. Ludwig RA. Toxin production by *Helminthosporium sativum* PK & B. and its significance in disease development. *Can J Bot*. 1957;35(3):291–303. <https://doi.org/10.1139/b57-026>.
23. Han J, Zhang J, Song Z, Liu M, Hu J, Hou C, et al. Genome- and MS-based mining of antibacterial chlorinated chromones and xanthenes from the phytopathogenic fungus *Bipolaris sorokiniana* strain 11134. *Appl Microbiol Biotechnol*. 2019;103(13):5167–81. <https://doi.org/10.1007/s00253-019-09821-z>.
24. Wang J, Chitsaz F, Derbyshire MK, Gonzales NR, Gwadz M, Lu S, et al. The conserved domain database in 2023. *Nucleic Acids Res*. 2023;51(D1):D384–8. <https://doi.org/10.1093/nar/gkac1096>.
25. Blin K, Shaw S, Augustijn HE, Reitz ZL, Biermann F, Alanjary M, et al. antiSMASH 7.0: new and improved predictions for detection, regulation, chemical structures and visualisation. *Nucleic Acids Res*. 2023;51(W1):W46–50. <https://doi.org/10.1093/nar/gkad344>.
26. Huaran Z, Haiyan Z, Yuqi H, Yi Z. Genome mining reveals the biosynthesis of sativene and its oxidative conversion to seco-sativene. *Org Lett*. 2024;26(1):338–43. <https://doi.org/10.1021/acs.orglett.3c04005>.
27. Abdel-Lateff A, Okino T, Alarif WM, Al-Lihaibi SS. Sesquiterpenes from the marine algalicolous fungus *Drechslera* sp. *J Saudi Chem Soc*. 2013;17(2):161–5. <https://doi.org/10.1016/j.jscs.2011.03.002>.
28. Fan Y-Z, Tian C, Tong S-Y, Liu Q, Xu F, Shi B-B, et al. The antifungal properties of terpenoids from the endophytic fungus *Bipolaris eleusines*. *Nat Prod Bioprospect*. 2023;13(1):43. <https://doi.org/10.1007/s13659-023-00407-x>.
29. Osterhage C, König GM, Höller U, Wright AD. Rare sesquiterpenes from the algalicolous fungus *Drechslera dematioidea*. *J Nat Prod*. 2002;65(3):306–13. <https://doi.org/10.1021/np010092l>.
30. Li Z-H, Ai H-L, Yang M-S, He J, Feng T. Bioactive sativene sesquiterpenoids from cultures of the endophytic fungus *Bipolaris eleusines*. *Phytochem Lett*. 2018;27:87–9. <https://doi.org/10.1016/j.phytol.2018.07.007>.
31. Grimblat N, Zanardi MM, Sarotti AM. Beyond DP4: an improved probability for the stereochemical assignment of isomeric compounds using quantum chemical calculations of NMR shifts. *J Org Chem*. 2015;80(24):12526–34. <https://doi.org/10.1021/acs.joc.5b02396>.
32. Zhang L, Liu X, Zhang J, Jiang L, Zhu G, Han J, et al. Preparation method of helminthosporol type sesquiterpenoids and its preparation method thereof. *ZL201910566725X*; 2019.
33. Tamura S, Sakurai A. Syntheses of several compounds related to helminthosporol and their plant growth-regulating activities. *Agric Biol Chem*. 2014;28(5):337–8. <https://doi.org/10.1080/00021369.1964.10858247>.
34. Nakajima H, Isomi K, Hamasaki T, Ichinoe M. Sorokinianin—a novel phytotoxin produced by the phytopathogenic fungus *Bipolaris sorokiniana*. *Tetrahedron Lett*. 1994;35(51):9597–600. [https://doi.org/10.1016/0040-4039\(94\)88520-6](https://doi.org/10.1016/0040-4039(94)88520-6).
35. Lodewyk MW, Gutta P, Tantillo DJ. Computational studies on biosynthetic carbocation rearrangements leading to sativene, cyclosativene, α -ylangene, and β -ylangene. *J Org Chem*. 2008;73(17):6570–9. <https://doi.org/10.1021/jo800868r>.
36. Phan C-S, Li H, Kessler S, Solomon PS, Piggott AM, Chooi Y-H. Bipolenins K-N: New sesquiterpenoids from the fungal plant pathogen *Bipolaris sorokiniana*. *Beilstein J Org Chem*. 2019;15:2020–8. <https://doi.org/10.3762/bjoc.15.198>.
37. Nakajima H, Toritsu Y, Fujii Y, Ichinoe M, Hamasaki T. Biosynthesis of sorokinianin a phytotoxin of *Bipolaris sorokiniana*: evidence of mixed origin from the sesquiterpene and TCA pathways. *Tetrahedron Lett*. 1998;39(9):1013–6. [https://doi.org/10.1016/S0040-4039\(97\)10803-6](https://doi.org/10.1016/S0040-4039(97)10803-6).
38. Steele CL, Crock J, Bohlmann J, Croteau R. Sesquiterpene synthases from grand fir (*Abies grandis*). Comparison of constitutive and wound-induced activities, and cDNA isolation, characterization, and bacterial expression of delta-selinene synthase and gamma-humulene synthase. *J Biol Chem*. 1998;273(4):2078–89. <https://doi.org/10.1074/jbc.273.4.2078>.
39. Elisashvili V. Submerged cultivation of medicinal mushrooms: bioprocesses and products (review). *Int J Med Mushrooms*. 2012;14(3):211–39. <https://doi.org/10.1615/IntJMedMushr.v14i3.10>.
40. Ulrike L, Niedermeyer THJ, Wolf-Dieter J. The pharmacological potential of mushrooms. *Evid Based Complement Altern Med*. 2005;2(3):285–99. <https://doi.org/10.1093/ecam/neh107>.
41. Li Y-Y, Tan X-M, Yang J, Guo L-P, Ding G. Naturally occurring seco-sativene sesquiterpenoid: chemistry and biology. *J Agric Food Chem*. 2020;68(37):9827–38. <https://doi.org/10.1021/acs.jafc.0c04560>.
42. Jiang L, Zhang X, Sato Y, Zhu G, Minami A, Zhang W, et al. Genome-based discovery of enantiomeric pentacyclic sesterterpenes catalyzed by fungal bifunctional terpene synthases. *Org Lett*. 2021;23(12):4645–50. <https://doi.org/10.1021/acs.orglett.1c01361>.
43. Jiang L, Zhu G, Han J, Hou C, Zhang X, Wang Z, et al. Genome-guided investigation of anti-inflammatory sesterterpenoids with 5–15 trans-fused ring system from phytopathogenic fungi. *Appl Microbiol Biotechnol*. 2021;105(13):5407–17. <https://doi.org/10.1007/s00253-021-11192-3>.
44. Ruggeri FM, Frisch M, Trucks G, Schlegel H, Scuseria G, Robb M, et al. Gaussian 03, Revision E01; 2004.
45. Cammi R, Tomasi J. Remarks on the use of the apparent surface charges (ASC) methods in solvation problems: iterative versus matrix-inversion procedures and the renormalization of the apparent charges. *J Comput Chem*. 1995;16(12):1449–58. <https://doi.org/10.1002/jcc.540161202>.
46. Yang G-X, Ge S-L, Wu Y, Huang J, Li S-L, Wang R, et al. Design, synthesis and biological evaluation of 3-piperazinecarboxylate sarsasapogenin derivatives as potential multifunctional anti-Alzheimer agents. *Eur J Med Chem*. 2018;156:206–15. <https://doi.org/10.1016/j.ejmech.2018.04.054>.

Publisher's Note

Springer Nature remains neutral with regard to jurisdictional claims in published maps and institutional affiliations.